PHASE BEHAVIOR OF ALKANES IN SHALE NANOPORES

A Thesis

by

BEHNAZ RAHMANI DIDAR

Submitted to the Office of Graduate and Professional Studies of
Texas A&M University
in partial fulfillment of the requirements for the degree of

MASTER OF SCIENCE

Chair of Committee,	I. Yucel Akkutlu
Committee Members,	Hadi Nasrabadi
	Yalchin Efendiev
	Maria A. Barrufet
Head of Department,	A. Daniel Hill

May 2015

Major Subject: Petroleum Engineering

ABSTRACT

This thesis is an analysis of the effect of shale nanopore confinement on fluid phase behavior using Monte Carlo molecular modeling. Research conducted so far in this area in the oil and gas industry mainly encompasses single component fluids and sorption densities in few PVT conditions. Many outstanding questions exist such as the concept of fluid pressure in confinement, multi-component fluid sorption and phase behavior/transition in confinement and the effect of pore type, geometry and heterogeneity on sorption capacity, some of which this thesis aims to answer.

The confinement effect is first investigated for single component fluids using the grand canonical ensemble of Monte Carlo. In addition to phase diagram shifts, results show that in confinement the gas phase is affected greater than the liquid phase. It is shown that the three fluids of methane, n-butane and n-octane approach their bulk behavior at approximately 12nm width slit-shaped confinements. The investigation is extended to multi-component fluids using the NPT-Gibbs ensemble Monte Carlo. It is concluded that in mixtures, light components affect and suppress the phase diagram greater than heavy components. Furthermore, some preliminary studies were also conducted in the area of fluid adsorption in SWCNT. Ultimately, it is concluded that current equations of state cannot accurately predict and describe fluid behavior in shale nanopores and therefore new correlations need to be sought for.

ACKNOWLEDGMENTS

In the conduct of this research, I was fortunate enough to be supplied by the wisdom, knowledge and help of many individuals. I cherish the energy and effort spent on this research, although hard at times. I treasure the lessons that I learned and people whom I met, including my colleagues and friends. I thank my committee members for supporting my work and providing their time to reviewing it. I am especially thankful to Dr. Khoa Bui for his insightful comments and extremely helpful lessons.

I am especially grateful and indebted to my advisor Dr. Yucel Akkutlu and his wife Pinar for their guidance and inspiration, and for their ideas, advice, and support in times of much need.

Finally, I am forever thankful to my family for their encouragement, love, and support in every conceivable manner.

NOMENCLATURE

a	Attraction parameter of the equation of state
a_1	Unit vector of graphene
a_2	Unit vector of graphene
b	Repulsion parameter of the equation of state
d	Diameter of carbon nanotube
k_B	Boltzmann constant
m	Integer
n	Integer
p	Momentum
r	Coordinate
C	Chiral vector
E	Total energy
N	Number of molecules
P	Pressure
P_c	Critical pressure
R	Universal gas constant
S	Entropy
T	Temperature
T_c	Critical temperature
U	Potential energy

V	Volume

Greek Symbols

α	Arbitrary maximum allowed displacement
β	$=1/k_BT$
ε	Energy scale of Lennard-Jones potential
μ	Chemical potential
ξ	Random number between 0 and 1
ρ	Density, g/cc
σ	Length scale of Lennard-Jones potential
ω	Pitzer shape factor
Δ	Spacing between graphene layers
H	Hamiltonian
K	Kinetic energy
P	Probability
Ω	Number of accessible microstates

GLOSSARY

DFT	Density Functional Theory
GCMC	Grand Canonical Monte Carlo
MANIAC	Mathematical Analyzer, Numerical Integrator and Computer
MFT	Mean Field Theory
MD	Molecular Dynamics
NPT	Isobaric-Isothermal Ensemble
NVT	Canonical Ensemble
PVT	Pressure-Volume-Temperature
SEM	Scanning Electron Microscopy
SWCNT	Single-Walled Carbon Nanotube
TraPPE	Transferable Potentials for Phase Equilibria
UA	United Atom
μVT	Grand Canonical Ensemble

TABLE OF CONTENTS

LIST OF TABLES

LIST OF FIGURES

FIGURE Page

CHAPTER I

INTRODUCTION

This thesis is an analysis of the effect of shale nanopore confinement on fluid phase behavior. The effect is first investigated for single component fluids and then expanded into multi-component fluids. Lastly, the pore geometry effect on fluid behavior is studied by comparing results of slit-shaped nanopores to those of carbon nanotubes. The analysis of any fluid system in nanoscale confinement in the laboratory is currently virtually impossible. The method utilized throughout this work is molecular simulation.

1.1 BACKGROUND

Scanning electron microscopy (SEM) images have shaped and immensely affected our understanding of shale. The resource shale is made up of both organic and inorganic matter. The portion of organic matter that is soluble in organic solvents is termed bitumen. The remaining portion that is insoluble in organic matter is called kerogen (Curtis et al., 2011a). Sondergeld et al. (2010) provided valuable and outstanding images, in some cases three-dimensional, of various shale samples in resolutions of up to 4-5nm wide pores. Such research revealed the extent of heterogeneity of pore structure even within a single shale formation. Loucks et al. (2009) analyzed pore samples from the Barnett shale using SEM and concluded that pores in shale are found in three categories; in discrete grains of organic matter, in disseminated organic matter and, in inorganic matter. They observed that pores are mainly in the nanoscale (‘nanopores’) and that the most common type of nanopores is found in the grains of organic material (kerogen). In the same work, they

directly relate origin of such pores to maturation of organic matter. They suggest that during thermal maturation in which kerogen is converted to hydrocarbons, liquid and gas coalesce into bubbles and form pores. Similarly, Curtis et al. (2011b) imaged Marcellus shale samples using SEM and studied the relationship between microporosity and thermal maturity.

The characterization of shale samples is mainly based on fluid intrusion or radiation techniques. Characterization is essential for understanding fluid storage and transport in shale. In a gas shale system, the gas is stored in two basic states; sorbed and free gas (Rahmani and Akkutlu, 2013; Rahmani, 2012; Ambrose et al., 2012; Montgomery et al., 2005). The term 'sorbed' refers to both adsorption onto surface of solid matter and absorption (dissolution) of gas. Currently, a precise distinction and quantification of these two forms of sorption does not exist. So far, the determination of total sorbed gas has relied mainly on adsorption and desorption studies of core and cutting samples (Clarkson et al., 2013; Adesida et al., 2011; Kang et al., 2011, Bustin et al., 2008). The total hydrocarbon in place in shale is undoubtedly an important matter in economic evaluation and field development planning. The methods currently used in the quantification of total gas storage are those that have been designed and applied for conventional resources and at best for coals. These methods require the sample to be cleaned and prepared for further analysis (e.g. adsorption measurements). Sample preparation procedures themselves are quite invasive and cause modification of the microstructure. For example, as discussed by Suleimenova et al. (2014), the traditional method of vacuum oven heating is used in the final step of kerogen isolation to remove all water from the sample. In this step, water

inside the pores is heated until it transitions to gas and leaves the pore. The surface tension of water transitioning to vapor exerts capillary stress on pore walls, forcing the pore shape to change. In the same work, critical point drying is suggested and tested as an alternative procedure for water removal to minimize destruction of microstructure. Apart from preparation, sample analysis may also be erroneous to some extent. For example, porosity measurement of a confined sample simulating reservoir stress conditions is currently very difficult to obtain if not impossible (Bustin et al., 2008). In addition, in many instances the reservoir temperature and pressure to be simulated are very high and exceed the instrumental limits. Nonetheless, methods used so far have established valuable and instructive insight into the unknowns of shale.

The phase behavior of fluid is of significant importance in production from shale. Experimental methods on fluid phase behavior are less applicable to the nanopores of shale. Much of the knowledge that exists in this area is gained from theoretical methods and molecular simulation investigations. Research in this area using molecular simulation is well-established and documented in other industries such as material science, chemicals and pharmaceuticals. Zarragoicoechea and Kuz (2002, 2004) theoretically studied the behavior of fluid in nanopores with inert walls via an extension of the van der Waals equation of state and found results to be in good agreement with numerical simulations and experimental data. Diaz-Campos et al. (2009) pioneered the use of molecular simulations in the oil and gas industry to study solubility of methane in water within confinement. Rahmani and Akkutlu (2013) have investigated the adsorption of methane and light alkane mixtures in slit-shaped carbon nanopores. Mosher et al. (2013), Firouzi

and Wilcox (2012) and Liu and Wilcox (2012) have also investigated the adsorption of methane and/or carbon dioxide in micro- and mesopores through molecular simulations with application to carbon capture and sequestration. Fluid behavior in nanopore confinement is now widely known to deviate from bulk state (Singh et al. 2010; Singh et al. 2009; Jiang et al. 2005; Gelb et al. 1999). Research conducted so far in the oil and gas industry mainly encompasses single component fluids and at most covers sorption densities in few PVT conditions. Many outstanding questions exist such as the concept of fluid pressure in confinement, multi-component fluid sorption and phase behavior/transition in confinement and the effect of pore type, geometry and heterogeneity on sorption capacity, some of which this thesis aims to answer.

1.2 STATEMENT OF PROBLEM

So far in the oil and gas industry, in our efforts to study and understand fluid phase behavior in confinement, methods have been introduced and used that are solely based on experiments. While these methods have contributed immensely to our knowledge in this area, some shortcomings exist that necessitate the development of new methods. In this respect, there are methods that have been used in other industries for many years but have only recently found their way into the oil and gas industry. With the advances in computers and technology in the past few decades, molecular simulations have risen and contributed to our studies and proven to be a reliable method. In comparison to bulk state fluids, confined fluids have received far less attention, especially in the oil and gas industry. While the topic may seem fairly straightforward, underlying complexities have prevented the fast progress in the area. First, molecular simulations whether Monte Carlo

or molecular dynamics, are purely based on theoretical methods and computational techniques. These calculations can be performed by hand for simple systems but are too cumbersome for many-body systems and therefore require computerized algorithms at the expense of computation time that subsequently require optimization. Second, molecular simulations require parameters to mimic the fluid of investigation in the atomistic level. No physical experiments exist to accommodate molecular simulations with such parameters. In fact, only molecular simulations in the atomistic level (ab initio calculations) can provide such data to those in the molecular level. The reliability of results obtained from molecular modeling depends on parameters used for the system. Dedication of research to finding and evaluating such parameters is vast and ongoing. Third, assuming correct parameters and optimized algorithms are used, careful analysis and interpretation of results does not seem to be an easy task either. Searching for trends in an ocean of data corresponding to an array of temperatures, pressures and compositions is comparable to solving a thousand-piece jigsaw puzzle. Nevertheless, molecular modeling is a robust method that has helped predict the behavior of many fluids including those hypothetical.

This thesis uses this method and begins by revisiting phase behavior of single component fluid in confinement. New results are documented in this thesis that do not necessarily accord with those published elsewhere. The multiple-composition nature of oil and gas directs the study of multi-component fluid in confinement. Complexities arise from pore wall selectivity and therefore fluid heterogeneity that pose a challenge to the study of multi-component fluid in confinement. A new methodology is developed, tested and discussed in this thesis that overcomes this challenge. Finally, after studying single

and multi-component fluid in slit-shaped pore, it is tempting to see whether this behavior would be affected by other pore geometries (e.g. nanotube) and if so, to what degree.

1.3 RESEARCH OBJECTIVES

This thesis focuses on understanding the true behavior of fluid in nanopore confinement using molecular simulations first by studying single component fluids and then by moving on to mixtures. Due to the complexities arising from fluid composition heterogeneity in nanopores, a new methodology is developed to study fluid mixtures. Therefore the objectives of the research are as follows:

a) Evaluating correct molecular simulation technique and parameters for bulk single-component fluid and thereof modeling the fluid with those obtained parameters in nanopore confinement.

b) Demonstrating the compositional heterogeneity of multi-component fluid in nanopores and thereof developing a new methodology for dealing with such systems.

c) Studying the effect of nanopore geometry on fluid adsorption and phase behavior.

1.4 METHOD OVERVIEW

Molecular simulations have emerged as a reliable method to investigate various phenomena and properties of fluids where experiments are no longer applicable. Equilibrium properties of fluid can be obtained by either Monte Carlo or molecular dynamics method. The difference between these two methods is that Monte Carlo generates configurations based on appropriate probability distribution for a statistical

ensemble whereas molecular dynamics finds such configurations by solving Newton's equations of motion. In each of the two methods, there are many techniques and algorithms that have been developed over the years to accommodate research on various aspects such as fluid transport, phase equilibrium and transition. In the study of phase behavior, the Monte Carlo method is the method of choice. In this method, three main ensembles are devised; NPT, NVT (canonical) and μVT (grand canonical), each of which has at least one extensive variable (N or V). In each of the three ensembles, the fixed input variables are those that the ensemble is named by and the other variables are outputs. For example, in the NPT ensemble, the number of molecules N, pressure P and temperature T are the fixed input variables and volume V and chemical potential μ are outputs of the simulation. Within the Monte Carlo realm, the Gibbs ensemble methodology and the grand canonical ensemble are used for the study of fluid phase equilibrium. As will be explained in subsequent chapters, the grand canonical ensemble and the Gibbs ensemble methodology will be used for single component and multi-component fluid systems, respectively.

Since its advent, molecular simulation has been used and tested extensively to study properties of fluids in their bulk state. Simulation methodologies and techniques have improved and shown good agreement with experimental data. As such, molecular simulation has also been used to predict fluid properties at conditions that are inaccessible in the laboratory. Despite the vast attention that has been given to bulk state fluid, the investigation into confined fluid is relatively new. Nonetheless, thanks to the chemical and energy industry, the need for understanding the true nature of fluid in nanoscale confinement has grown markedly. In the unconventional resources sector of the oil and

gas industry, we frequently encounter conditions of unusually high temperature and pressures. The pore size in such resources is also virtually always in the nanometer scale. In our dealings with such conditions, molecular simulations have gained significant attention.

The research work in this thesis has been based entirely upon molecular simulations. In molecular simulation, different ensembles and methodologies are devised to serve different aspects and problems. The validity and accuracy of results obtained from molecular simulation rely on factors such as the choice of ensemble, methodology and, simulation and fluid parameters. Over the years, fluid models and parameters have been perfected to give accurate results. Methodologies and algorithms have also been developed to accommodate the investigation of certain cases. In this thesis, a new methodology within the molecular simulation realm has been developed to study multi-component fluid behavior in nanopore confinement. This methodology is explained in chapter 3. In chapters 2 and 4, a different but well-established ensemble has been utilized to study single component fluids in confinement.

1.5 THESIS OUTLINE

This thesis is organized in five chapters. Background and literature review, statement of problem, research objectives and methodology overview constitute chapter 1. Chapter 2 explains the procedure used for molecular modeling of single component *n*-alkanes in slit-shaped nanopore and discusses the results obtained. In chapter 3, the issue of multi-component fluids in slit-shaped nanopores is approached and a methodology is developed and used to study the phase behavior of binary and ternary alkane mixtures.

Chapter 4 is a study of pore geometry effect on adsorption. Methane is modeled in a single wall carbon nanotube (SWCNT) under several conditions. Results are compared to those obtained from the same fluid in slit-shaped pore. Lastly, chapter 5 discusses the findings of this research and their implications.

CHAPTER II

SINGLE COMPONENT ALKANES IN NANOPORES

Single component fluids, including *n*-alkanes, have been studied generously in the literature both theoretically and experimentally. Recently, the confinement of such fluids has gained attention. The focus of this chapter is to revisit and study three *n*-alkanes (methane, n-butane and n-octane) in slit-shaped graphite nanopores using molecular simulations. The ensemble used and the modeling setup is described. Correct fluid parameters are found by reproducing experimental data of bulk thermodynamic properties. Phase diagrams of the three fluids are obtained in various nanopore sizes. The upper limit of where nanopore effect is seen in each fluid is also reported.

2.1 INTRODUCTION

The confinement of single component fluids such as CO_2, N_2 and alkanes has been studied as early as the 1980's. The earliest studies in which molecular simulations were employed were mainly focused on the adsorption of these fluids onto pores of zeolite, graphite and mica material with applications to carbon capture and global warming mitigation and, gas separation and purification (Cracknell et al., 1995; Cracknell and Nicholson, 1994; Kaneko et al., 1994; Tan and Gubbins, 1992; Van Tassel et al., 1992; Razmus and Hall, 1991). These investigations identify some important features of adsorption. For example, Cracknell and Nicholson (1994) use Grand Canonical Monte Carlo simulations to model the adsorption of methane and ethane in graphite slit-shaped pores. In that work, the ethane is modeled as a more realistic two-site molecule rather than

a single-sited sphere. The selectivity of the pore walls to favor and adsorb one fluid to the other is discussed and measured. The effect of pore size, temperature and bond length (two-sited ethane model vs. spherical) on selectivity is also evaluated. Selective adsorption of fluids is important in fields such as tertiary oil recovery and, carbon capture and storage.

Apart from adsorption, phase transition in confinement has also been addressed by many researchers. Molecules of a fluid, when confined within narrow pores of a few molecular diameters wide, exhibit peculiar behavior such as layering otherwise not seen in bulk conditions. The walls of such pores exert force on fluid molecules, and create competition between fluid-wall and fluid-fluid forces leading to interesting surface-driven phenomena such as shifts in phase transitions. For a bulk fluid, phase transition is usually seen as a sharp change in the density or composition. In addition, at transition point, chemical potential and free energies of the two phases are equal. However, for a confined fluid, care must be taken in our definition and evaluation of phase transition (Gelb et al., 1999).

In the family of theoretical methods applicable for the study of confined fluid phase transitions, the density functional theory (DFT) and Monte Carlo molecular simulations are among the most widely-used. The Monte Carlo method was developed by Ulam, von Neumann, Metropolis and coworkers in the Los Alamos National Laboratory and launched on the MANIAC, one of the first digital computers (Anderson, 1986). Over the next years, Metropolis et al. (1953) introduced and used the Monte Carlo method and set up their system of reasonable amount (sufficient for computers of the time) of particles N, in a fixed volume V, at a fixed temperature T (hence the NVT or canonical ensemble)

to investigate, for the first time, the equation of state for a liquid (Frenkel, 2004). In that work, they also described a new scheme, the importance sampling, to generate new configurations more efficiently. Apart from the NVT ensemble, there exists another ensemble in Monte Carlo, the grand canonical (GCMC), which is especially suited for adsorption and phase behavior studies. GCMC uses the Markov chain to generate configurations of molecules within a fluid with the correct density and energy distribution. Each step of the Markov chain is generated by modifying the current molecular configuration and calculating the density and energy of the new configuration. This modification is achieved in three basic ways: inserting a new molecule in a random position (insertion move), deleting an existing molecule from a random position (deletion move), and displacing an existing molecule by a random length and direction (displacement/translation move). As will be discussed later in this section, these moves are then accepted or rejected according to set temperature and chemical potential (hence μVT) criteria. This means that at the end of each move or cycle of moves, temperature, chemical potential and energy of the system need to be calculated. A fundamental question here is: how are density, energy and other thermodynamic parameters calculated for a many-body system?

In statistical mechanics, the average of any variable A of N particles is expressed as a function of coordinate r and momentum p by

$$\langle A \rangle = \frac{\int dp^N dr^N A(p^N,r^N) \exp[-\beta H(p^N,r^N)]}{\int dp^N dr^N \exp[-\beta H(p^N,r^N)]} \tag{2.1}$$

where $\beta = \frac{1}{k_B T}$ and k_B is the Boltzmann constant. H is the Hamiltonian of the system and H=K+U, where K is the kinetic and U is the potential energy of the system. In Monte Carlo method, momentum of a particle is not dealt with. Then Equation 2.1 becomes:

$$\langle A \rangle = \frac{\int dr^N \exp[-\beta U(r^N)] A(r^N)}{\int dr^N \exp[-\beta U(r^N)]} \tag{2.2}$$

The term $\exp(-\beta U)$ is the Boltzmann factor. This means if the positions of particles in a many-body system are known, then for example, the energy of the system can be calculated. Note that Equation 2.2 implies that the average of a variable is the sum of all the probability densities of the system configurations multiplied by the value of the variable at each of those configurations.

Obviously, the multi-dimensional calculation in Equation 2.2 for a many-body system cannot be performed by any computer. To solve this problem, Metropolis et al. (1953) prescribed the importance sampling scheme (also known as the Metropolis scheme) that was mentioned earlier. In this scheme, rather than randomly choosing configurations, configurations are chosen proportional to and with a probability of the Boltzmann factor. In other words, those configurations are chosen that have a non-negligible value of $\exp(-\beta U)$, hence the importance sampling. In the following, the procedure for the importance sampling is described.

First, each particle is moved by an $\alpha\xi$ amount, where α is the arbitrary maximum allowed displacement and ξ is a random number between 0 and 1. The change in total energy of the system at the end of the move is then calculated. If the move would bring the system to a lower state of energy, the move is accepted. If the move would bring the system to a

higher state of energy, another random number ξ is generated and the move is only accepted if $\xi < \exp(-\beta U)$. Thus, the Ma rkov chain is formed and the system is merged to equilibrium. It is worth noting that equilibrium implies thermal (T), chemical (μ) and mechanical (P) equilibrium throughout the fluid. Thermal and chemical equilibrium is readily achieved by the grand canonical input setup. The remaining criterion, mechanical equilibrium, is also achieved by the rigorously demonstrated fact that constant chemical potential, which is the case for fluid throughout the pore, implies mechanical equilibrium of an inhomogeneous fluid (Henderson, 1983).

The mentioned Markov chain utilizing importance sampling is used in all ensembles of Monte Carlo simulations. However, in the GCMC, another underlying method exists which is discussed in the following.

In statistical analysis of a many-body system, the accessible states of the system (microstates) in the journey to equilibrium and the probability of finding the system in those states are enumerated (Hoch, 2011). In equilibrium, all accessible microstates of the system occur with equal probability. A system which is not in equilibrium will continue evolving between configurations and microstates until it arrives at equal probabilities. The configurations in an ensemble are in the same macrostate but can be found in different microstates. If the total number of accessible microstates with energy E of a system is $\Omega(E)$, then from statistical physics and thermodynamics we have:

$$S = k_B \ln(\Omega(E)) \tag{2.3}$$

where S is entropy. The probability of finding the system in a certain microstate with energy E, volume V and number of particles N is then:

$$P = \frac{1}{\Omega(E, V, N)} = \exp(-\frac{S}{k_B}) \tag{2.4}$$

The entropy S of a system is a function of energy E, volume V and number of particles N:

$$S = S(E, V, N) \tag{2.5}$$

Then,

$$dS = \left(\frac{\partial S}{\partial E}\right)_{V,N} dE + \left(\frac{\partial S}{\partial V}\right)_{E,N} dV + \left(\frac{\partial S}{\partial N}\right)_{E,V} dN \tag{2.6}$$

And,

$$dS = \frac{1}{T} dE + \frac{P}{T} dV - \frac{\mu}{T} dN \tag{2.7}$$

In the μVT ensemble, volume V of the system remains unchanged (dV=0). Therefore, Equation 2.7 becomes:

$$dS = \frac{1}{T}(dE - \mu dN) \tag{2.8}$$

Equation 2.4 can now be written as:

$$P = \exp\left(-\frac{ST}{k_B T}\right) = \exp(-\beta ST) \tag{2.9}$$

And finally:

$$P = \exp[-\beta(E - \mu N)] \tag{2.10}$$

In the process of reaching equilibrium, as mentioned earlier, a probability distribution is obtained for the system. At equilibrium, the probability of occurrence of all microstates is equal. After equilibrium is reached, thermodynamic properties of interest are obtained by averaging their microscopic counterparts over all configurations.

As discussed earlier, phase transition is accompanied by an abrupt change in properties such as density and composition. At this point, chemical potential and free energy of the two phases are equal. At critical point however, while chemical potential and free energies remain equal, the probability of finding the system at both phases are also equal (phase coexistence). In other words, the critical point would appear as two equal-height peaks on the probability distribution of the system, each peak corresponding to one phase. This key feature is the basis of the histogram reweighting method which is coupled with GCMC to obtain critical parameters of a fluid. Histogram reweighting was first applied to phase transition studies by Ferrenberg and Swendsen (1989). In this method, over a course of a GCMC simulation, a histogram of probability distributions for a certain temperature and chemical potential is obtained. This histogram is then reweighted to other values of temperature and chemical potential by simply dividing the probability in one set of temperature and chemical potential to that of another:

$$\frac{P_1}{P_2} = \exp\big((\beta_1\mu_1 - \beta_2\mu_2)N\big) \times \exp(-(\beta_1 - \beta_2)E) \tag{2.11}$$

Or

$$\ln P_1 = \ln P_2 + N(\beta_1\mu_1 - \beta_2\mu_2) - E(\beta_1 - \beta_2) \tag{2.12}$$

The discussed method has been used widely in the phase behavior, surface tension and especially critical point determination of confined fluids as well as bulk (Singh et al. 2009 and 2010; Singh and Errington, 2006; Potoff and Siepmann, 2001; Potoff and Panagiotopoulos, 2000 and 1998; Panagiotopoulos, 2000). This method has been used in this chapter to construct and study the phase diagram of three *n*-alkanes in graphite slit

nanopores in various sizes. Figure 2.1 shows an example of the bimodal probability distribution at critical point for n-butane in a 4nm slit-pore, obtained in this thesis.

2.2 SIMULATION METHOD

2.2.1 Methane

2.2.1.1 Simulation Setup

In section 2.1 it was discussed that the Markov chain in Monte Carlo simulations generates a sequence of configurations of the system with a probability proportional to the Boltzmann factor which depends on the potential energy of the system. This potential energy of the system consists of intermolecular and intramolecular interactions that are described in the subsequent sections of fluid and pore models. The system of methane in bulk or nanopore in the GCMC is set up in one computational box with fixed volume V and temperature T. The chemical potential μ of methane is also a fixed input to the simulation. A maximum number of molecules are initially set up in the box. These molecules are allowed to exit, enter, rotate and/or displace within the box. A total of at least 4×10^6 moves are performed. Histograms of probability densities with respect to number of molecules are collected for every 2×10^5 move. Histograms are then analyzed. Critical points are identified as values of temperature and chemical potential where the probability density exhibited two equal peaks. The GCMC simulation setup and parameters for methane were first validated by running the model in bulk state and comparing to experimental data. Methane was then placed and modeled in slit-pores of various widths.

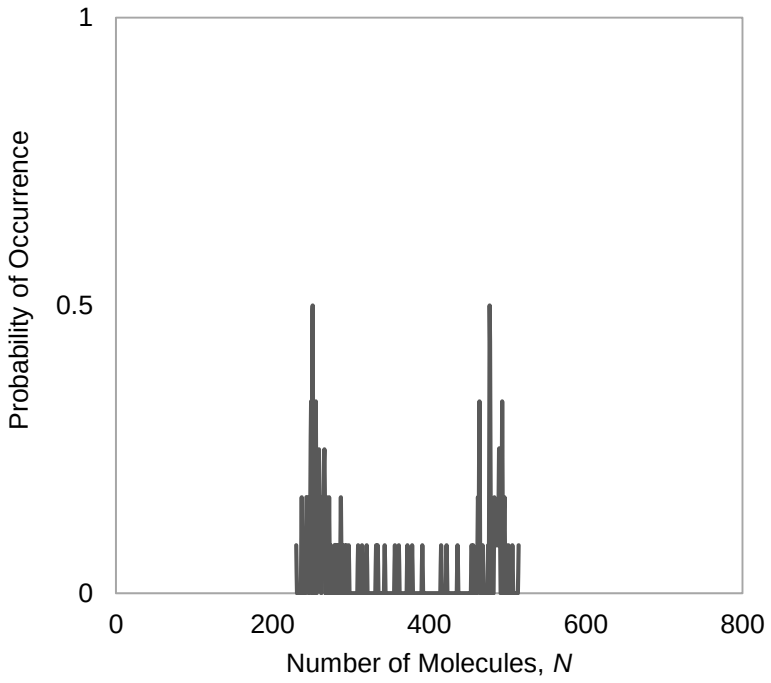

Figure 2.1: Probability distribution of n-butane in 4nm graphite slit-pore at critical point, obtained from GCMC simulation in this work.

2.2.1.2 Fluid Model

The methane molecule is modeled as a spherical site (CH4) using the TraPPE-UA force field. The Transferrable Potentials for Phase Equilibria (TraPPE) force field was developed and introduced by the Siepmann statistical mechanics research group in 1998 (Martin and Siepmann, 1998). In the United-Atom (UA), groups such as methyl and methylene are treated as one site. For instance, methane is treated as one site (CH_4), ethane as two sites (two $–CH_3$ groups), n-butane as four sites (two $–CH_3$ and two $–CH_2$-) and so on. Force fields are developed by ab initio calculations and contain information pertaining to atomic mass, bond pattern length and angle and, potential coefficients of various molecules or particle sites. The interaction of two sites i and j of different molecules (non-bonded sites) within the fluid is described and calculated by the 12-6 Lennard-Jones potential:

$$U_{ij}(r_{ij}) = 4\varepsilon_{ij}\left[\left(\frac{\sigma_{ij}}{r_{ij}}\right)^{12} - \left(\frac{\sigma_{ij}}{r_{ij}}\right)^{6}\right] \tag{2.13}$$

where σ_{ij} and ε_{ij} are the length and energy scale of the Lennard-Jones interaction between two methane molecules i and j separated by a distance r_{ij}.

The cutoff radius of fluid particle interactions is chosen to be 15Å, beyond which the non-bonded potentials are no longer computed

2.2.1.3 Pore Model

The pore is modeled as box with two parallel slit-shaped graphite walls. The box is periodic in the x and y direction and fixed in z the direction where the walls are placed on either side. The interaction between the pore wall and fluid molecules is described by

the Steele Wall potential (Steele, 1973). This potential places a 10-4 Lennard-Jones potential on the pore wall by:

$$U(z) = 2\pi\varepsilon_{ij}\rho_j\sigma_{ij}^2\Delta\left[\frac{2}{5}\left(\frac{\sigma_{ij}}{z}\right)^{10} - \left(\frac{\sigma_{ij}}{z}\right)^{4} - \frac{\sigma_{ij}^4}{3\Delta(z+0.61\Delta)^3}\right] \quad (2.14)$$

Here, σ_{ij} and ε_{ij} are interaction parameters between fluid sites or molecules i and the wall j. These parameters are chosen here to be calculated by the Lorentz-Berthelot mixing rule:

$$\sigma_{ij} = \frac{\sigma_{ii} + \sigma_{jj}}{2} \quad (2.15a)$$

$$\varepsilon_{ij} = \sqrt{\varepsilon_{ii}\varepsilon_{jj}} \quad (2.15b)$$

The parameters σ_{ii} and ε_{ii} are included and given in the TraPPE-UA force field and, σ_{jj} and ε_{jj} represent parameters of the wall molecules. The values for σ_{ii} and ε_{ii} are listed in Table 2.1. Also ρ, Δ and z are parameters for the density of atom constituting the wall, parameter for the spacing between the layers in the wall and, distance between the two parallel walls, respectively. The pore walls are graphite walls and each wall consists of 3 layers of carbon molecules (graphene).

2.2.2 N-Butane

2.2.2.1 Simulation Setup, Fluid Model and Pore Model

The setup and pore model used for methane, described in section 2.2.1.1, is also used for n-butane. The n-butane molecule is modeled with the TraPPE-UA force field as four sites: two –CH3 (methyl) and two –CH2- (methylene), with Lennard-Jones interactions. The cutoff radius of fluid particle interactions is chosen to be 20Å.

Table 2.1: Lennard-Jones parameters of molecules present in the simulations.

Atom/molecule	Force field	ε/k_B, K	σ, nm
Carbon(wall)		28.0	0.340
CH4	TraPPE-UA	148.0	0.373
-CH3 group	TraPPE-UA	98.0	0.375
-CH2- group	TraPPE-UA	46.0	0.395

2.2.3 N-Octane

2.2.3.1 Simulation Setup, Fluid Model and Pore Model

The setup and pore model used for methane, described in section 2.2.1.1, is also used for n-octane. The n-octane molecule is modeled with the TraPPE-UA force field as eight sites: two –CH3 (methyl) and six –CH2- (methylene), with Lennard-Jones interactions. The cutoff radius of fluid particle interactions is chosen to be 20Å.

2.3 RESULTS

In the tiny space inside nanopores, the force exerted by the wall on the fluid molecules becomes decisive in the fluid behavior. As discussed by Ambrose et al (2010) and Rahmani and Akkutlu (2013), the fluid inside the pore forms a certain density profile. This profile shows two peaks of high density in the fluid layers adjacent to the walls reflecting high interaction between wall and fluid molecules. This can be explained as the following. Alkanes and graphite are both made up of carbon molecules. The carbon molecule has strong bonding energy which gives rise to the tendency of this molecule to form covalent bonds with other molecules. Obviously, in the small environment of a few nanometers, and therefore large surface area, this tendency is magnified. As fluid molecules compete to occupy the adjacent layer to the wall, the force exerted by the wall becomes screened, leaving other more inner layers of fluid molecules under lesser influence of the wall. From this, it can also be predicted that heavy longer-chained n-alkanes having more carbons, will be much more strongly attracted to the wall. This is the concept of selectivity. Many researchers have indeed confirmed this concept.

The notion of selectivity and density profile would imply transformation of a homogeneous fluid in bulk to that of a heterogeneous in nanopore confinement. It would also lead to peculiar consequences in the fluid phase behavior. To investigate this matter, first methane as the lightest alkane, n-butane as an intermediate alkane and finally n-octane as a heavy alkane are modeled in bulk state and obtained results are compared to the Peng-Robinson equation of state (Figure 2.2). Then, upon validation of the method, the three *n*-alkanes are modeled inside the pore. Results are shown in Figures 2.3, 2.4 and 2.5.

Note that the phase envelopes are plotted in the temperature-density plane. Beginning from the far left of the envelope and gradually moving right, the fluid is first in gas state. It then approaches the critical point at the envelope peak and is followed by the transition to liquid state.

2.4 DISCUSSION

The phase diagrams obtained from GCMC simulations for the three *n*-alkanes in their bulk state are in satisfactory agreement with the data extracted from Peng-Robinson equation of state to construct the bulk state diagram. This validates the simulation setup and the fluid model and allows the simulations to be performed in confinement with the pore model described earlier in section 2.2.1. Consequently, envelopes of these fluids in confinement are obtained and studied.

The obtained envelopes of confined alkanes show few important findings. First, in all three *n*-alkanes, critical point as well as the entire phase envelope is suppressed by confinement. This feature is observed in many studies of this sort. Second, the envelopes indicate that the left-hand-side (vapor/gas branch) of the fluid phase envelope is more

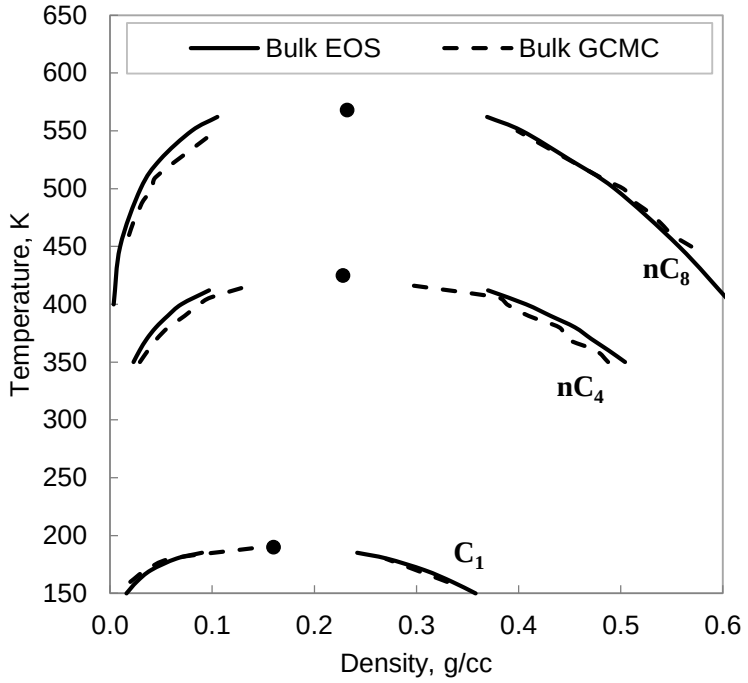

Figure 2.2: Phase diagrams of Bulk methane, n-butane and n-octane obtained from Peng-Robinson equation of state and GCMC simulations in this work. The dots indicate critical points.

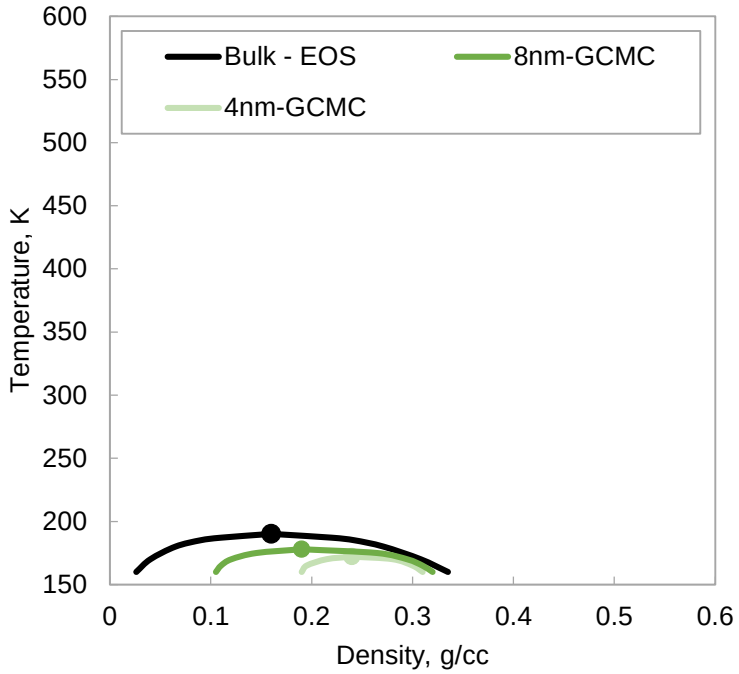

Figure 2.3: Phase diagrams of methane in graphite slit-pore of 4 and 8nm width obtained from GCMC simulations in this work and compared to bulk extracted from Peng-Robinson equation of state

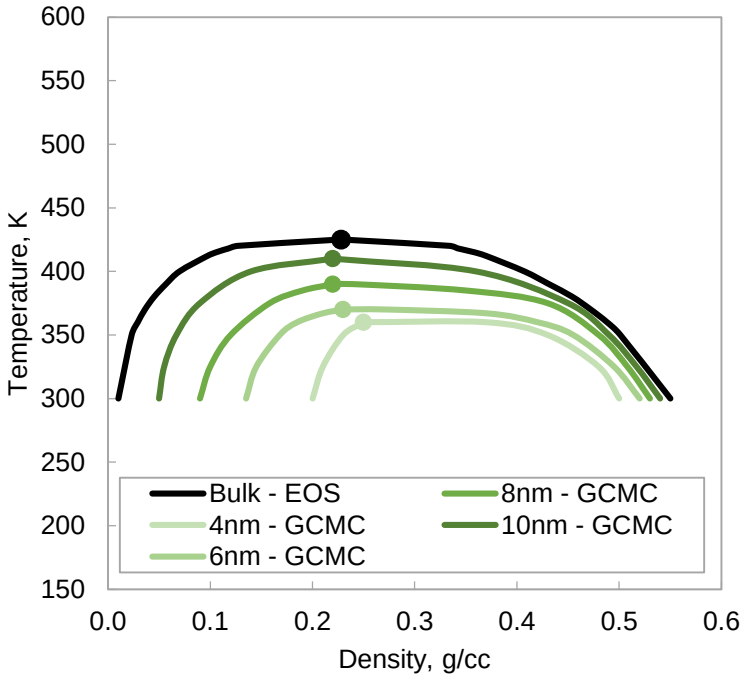

Figure 2.4: Phase diagrams of n-butane in graphite slit-pores of 4, 6, 8 and 10nm width obtained from GCMC simulations in this work and compared to bulk extracted from Peng-Robinson equation of state

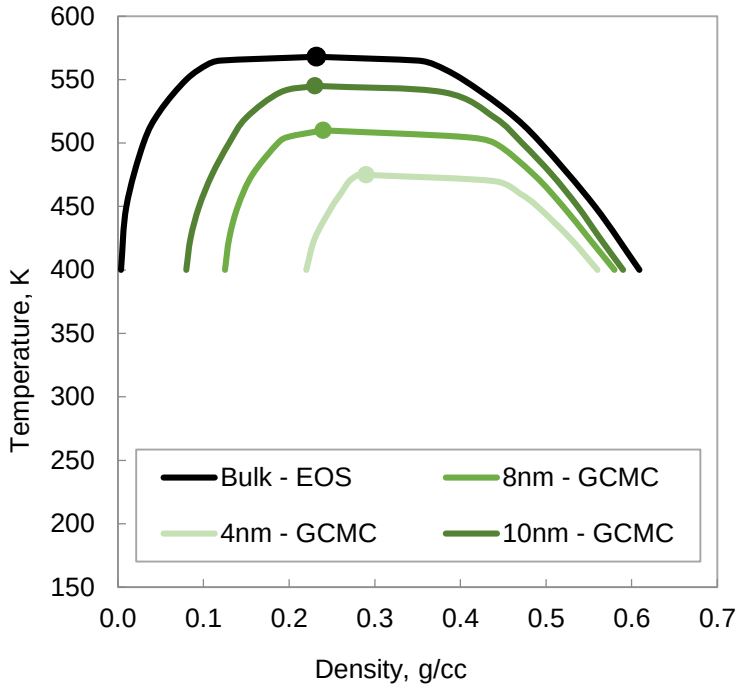

Figure 2.5: Phase diagrams of n-octane in graphite slit-pores of 4, 8 and 10nm obtained from GCMC simulations in this work and compared to bulk extracted from Peng-Robinson equation of state.

affected, than the right-hand-side (liquid branch), by confinement. The condition is more pronounced in smaller pores. This feature is not reported in other studies such as Singh et al. (2009) although it is observed in Singh et al. (2010) and Mi et al. (2006) for higher values of wall-fluid interaction potential depth parameter (equivalent to surface attraction). This parameter, as covered in section 2.2.1.3, is the geometric mean of the corresponding parameters for fluid-fluid and wall molecules interaction potentials and is obtained from ab initio calculations and included in the force field. The interaction potential depth parameter used in this thesis is based on the valid TraPPE-UA force field. Singh et al. (2009 and 2010) and Mi et al. (2006) studied phase envelopes without utilizing a specific force field and therefore used their own interaction parameters. Perhaps the main reason for the larger gap seen for the vapor branch of the envelopes is molecule layering. In smaller pores, layers are dominant throughout the pore and the walls are not allowing a free state for the molecules. Vapor transitions to liquid at much higher densities that is expected from bulk fluid. In larger pores, the envelope becomes more uniformly suppressed because apart from layers of molecules close to the wall, some, if not many, molecules are free from the grasp of the wall and can behave more similar to bulk state fluid. As for the liquid branch, by this time, complete layers of molecules have almost certainly formed and saturated close to the wall, insulating the inner layers from the wall and allowing a more bulk-like behavior of the fluid.

CHAPTER III

MULTI- COMPONENT ALKANE MIXTURES IN NANOPORES

Single component n-alkanes in confinement were studied in the previous chapter. The focus of this chapter is to study the mixture of those n-alkanes in slit-shaped graphite nanopores using molecular simulations. These mixtures, compared to single component fluids, can be more representative of the true multi-compositional nature of oil and gas. A methodology is described and used to deal with the heterogeneity of the fluid in confinement. The ensemble used and the modeling setup is described. Correct fluid parameters are found by reproducing experimental data of bulk thermodynamic properties. Phase diagrams of mixtures with various compositions are obtained in 4nm pore width.

3.1 INTRODUCTION

The adsorption of fluid mixtures in confinement and the concept of selectivity have been widely studied with theoretical and computer simulation techniques. Among the earliest are Sokolowski and Fischer (1990) who used DFT and molecular dynamics to study binary mixtures in slit-like pores. Kierlik and Rosinberg (1992) studied selectivity and the adsorption of binary mixtures in slit-shaped pores also using DFT. Cracknell et al. (1994 and 1995) studied adsorption and selectivity of CO_2/N_2, CO_2/CH_4 and CH_4/C_2H_6 mixtures in slit-shaped carbon nanopores using GCMC simulations. Such studies although enlightening, have not covered the phase behavior of mixtures in confinement. We can qualitatively predict, based on single component fluids that phase envelopes of mixtures will be affected by pore walls, but the extent of this effect is not yet clear.

In section 2.3 it was discussed how, due to layering, a single component fluid which is homogeneous in bulk transforms to a heterogeneous fluid in confinement. It was also discussed that a longer-chained alkane, having more carbons, would be more favored by the carbon wall than a shorter-chained. This would imply that for multi-component fluids, apart from a density profile parallel to the wall, a compositional profile meaning each layer of molecule having a different composition, would also appear, resulting in an inhomogeneous fluid. Due to this fact, the study of mixture phase behavior in confinement is beset with difficulty.

Aside from the grand canonical ensemble in Monte Carlo (GCMC), the NVT- and NPT-Gibbs ensembles are also widely used in phase behavior studies. The advantage of using these ensembles rather than the grand canonical is that our mixture can be studied at any temperature, pressure and volume of interest by directly entering their values as simulation inputs and without the need for previous knowledge of mixture properties such as the chemical potential. The 'Gibbs' part of these ensembles, attributed to J.W. Gibbs who originally derived phase equilibrium criteria in 1875, indicates that simulations are set up in two computational boxes. This methodology was first developed and used in the NVT ensemble by Panagiotopoulos (1987a) to directly calculate phase coexistence of bulk fluids by simulating each phase in one of the two boxes. Coupling the two boxes is equivalent to setting them in imaginary contact with each other in the absence of an interface. In equilibrium, temperature, pressure and chemical potential of the two phases are equal. In the Gibbs methodology, this is achieved by molecule and volume exchanges between the two boxes which are carried out in the Markov chain described earlier in

section 2.1. The NVT-Gibbs ensemble usually requires the total volume of the system of two boxes to be fixed while volumes are being exchanged with one another in the course of the simulation. Shortly after introducing the Gibbs methodology for phase equilibria studies in bulk, Panagiotopoulos (1987b) used the method for confined fluid in the same NVT ensemble. The system setup is described and validated as a fixed volume cylindrical-shaped pore inside a bulk single component fluid. The moves used, are displacement of molecules within (for internal equilibrium), as well as between (for chemical and therefore mechanical equilibrium) the pore and bulk fluid. No volume change moves were used. At the end of the simulation, the chemical potential of fluid inside the pore, regardless of a density profile existence, is equal to the chemical potential of the bulk fluid.

The method described in the mentioned work, was executed for a single component fluid. For a multi-component fluid, the only difference is in the criterion for chemical equilibrium; the chemical potential of each component in the pore would have to equal its correspondent in the bulk fluid box.

In the setup explained by Panagiotopoulos (1987b), bulk fluid box and pore volumes were kept constant. Therefore, a good prior knowledge of the total number of molecules for the setup is required. For a multi-component fluid, this becomes a major setback. The Gibbs methodology can alternatively be used in the NPT ensemble, since pressure is the conjugate thermodynamic variable of volume. In this ensemble, the bulk fluid box is now allowed to change volume to accommodate as many total numbers of molecules we wish to specify for the system. The NPT-Gibbs ensemble is used in the current chapter to obtain phase diagrams of alkane mixtures. The moves used are

displacement of molecules within and between the two boxes and volume changes of the bulk fluid. At the end of the simulation, the fluid inside the pore is in equilibrium with the bulk fluid. At this point, although each component of the fluid inside the pore forms a density profile across the pore width, not only is its chemical potential constant throughout the pore (internal chemical equilibrium) but it is also equal to that of the bulk fluid (Prausnitz et al., 1998[section 2.3, Pg17]). In addition, the condition for mechanical equilibrium between pore fluid and bulk fluid is unnecessary. If this were not true, as discussed by Panagiotopoulos (1987b), then the phase behavior of the fluid in an infinitely long slit-pore would be affected by the bulk fluid in contact with it. Since this is not the case, and the slit-pore is of fixed volume, then pressure need not be a variable for the systems equilibrium condition.

3.2 SIMULATION SETUP

The simulations performed here in the NPT-Gibbs ensemble are set up in two computational boxes; one is the slit-pore with fixed volume initially devoid of fluid, the other the bulk fluid with an initial composition, for example 50% of the total molecules belonging to CH_4 and the remaining 50% , to C_2H_6.

The total number of molecules N, temperature T and total system pressure P are kept constant in the simulation. Each simulation is run at a certain pressure. A total of at least 1×10^5 moves are performed where molecules are allowed to displace within and between boxes and, rotate about their center-of-mass. The volume of the bulk fluid box is also allowed to change. These runs are repeated for several many pressures (under same conditions) during which the state of the bulk fluid is carefully monitored for changes in

density. The exchange of molecules between the pore and bulk fluid box causes changes in the composition, although uniform, of the bulk fluid box. The importance of the bulk fluid box is that while it is in equilibrium with the pore fluid, it maintains a uniform composition and density all throughout. As such, by keeping track of the changes in this box, the pore fluid is indirectly monitored for changes in phase. The vapor-liquid equilibria and phase densities of the bulk fluid box are determined by the Peng-Robinson equation of state and the Extended Corresponding States model, respectively. At low pressures, the bulk fluid is in the vapor phase. As the pressure increases, the fluid first evolves to two-phase and then liquid. In the two instances that the fluid changes phase, the densities are recorded on the phase diagram for that temperature. This entire procedure is repeated for a number of temperatures, in increasing order, until dew- and bubble-point branches merge together at the critical point.

Fluids studied in this chapter are binary and ternary mixtures of methane, n-butane and n-octane. As in chapter 2, the pore here is also slit-shaped with two parallel graphite walls. Therefore, all fluid and pore parameters are the same as in section 2.3.

This simulation setup and parameters were first validated by running the model for two of the binary mixtures in bulk state and comparing to experimental data. Mixtures were then placed and modeled in slit-pores of 4nm width.

3.3 RESULTS

Mixtures of methane, ethane, n-butane and n-octane in confinement are studied with the setup explained earlier. All phase diagrams are plotted in the temperature-density plane and are compared to their bulk state obtained from the Peng-Robinson equation of

state. First, the method described is executed to validate the two 50%/50% mixtures of methane/ethane and methane/n-butane in bulk state (see Figure 3.1a and b). The figures show excellent agreement of the simulation results with those obtained from Peng-Robinson equation of state. Then, mixtures are studied in two main categories; 50%/50% and 90%/10%. These percentages are the initial simulation setup percentages (i.e. percentage of total molecules of one component initially in bulk fluid box) and are not weight percentages. Obviously, during the simulation, molecules are spread out between the two boxes as well as within and across the pore. Four binary mixtures are studied in those two categories; methane/ethane (Figure 3.1a), methane/n-butane (Figure 3.1b), methane/n-octane (Figure 3.1c) and ethane/n-octane (Figure 3.1d).

Due to wall selectivity, fluid composition plays an important role in the phase behavior in confinement. This role is evident from the diagrams in Figure 3.1. The effect is studied in two ways; by increasing the percentage of the lightest component from 50% to 90% in all four binaries and, by pairing the lightest component (methane) with ethane (lighter), n-butane (intermediate) and n-octane (heavy). In the case of methane/ethane mixture, the shift in the phase diagram of the mixture is not significant, although a slight shift in the 90%/10% case can be detected.

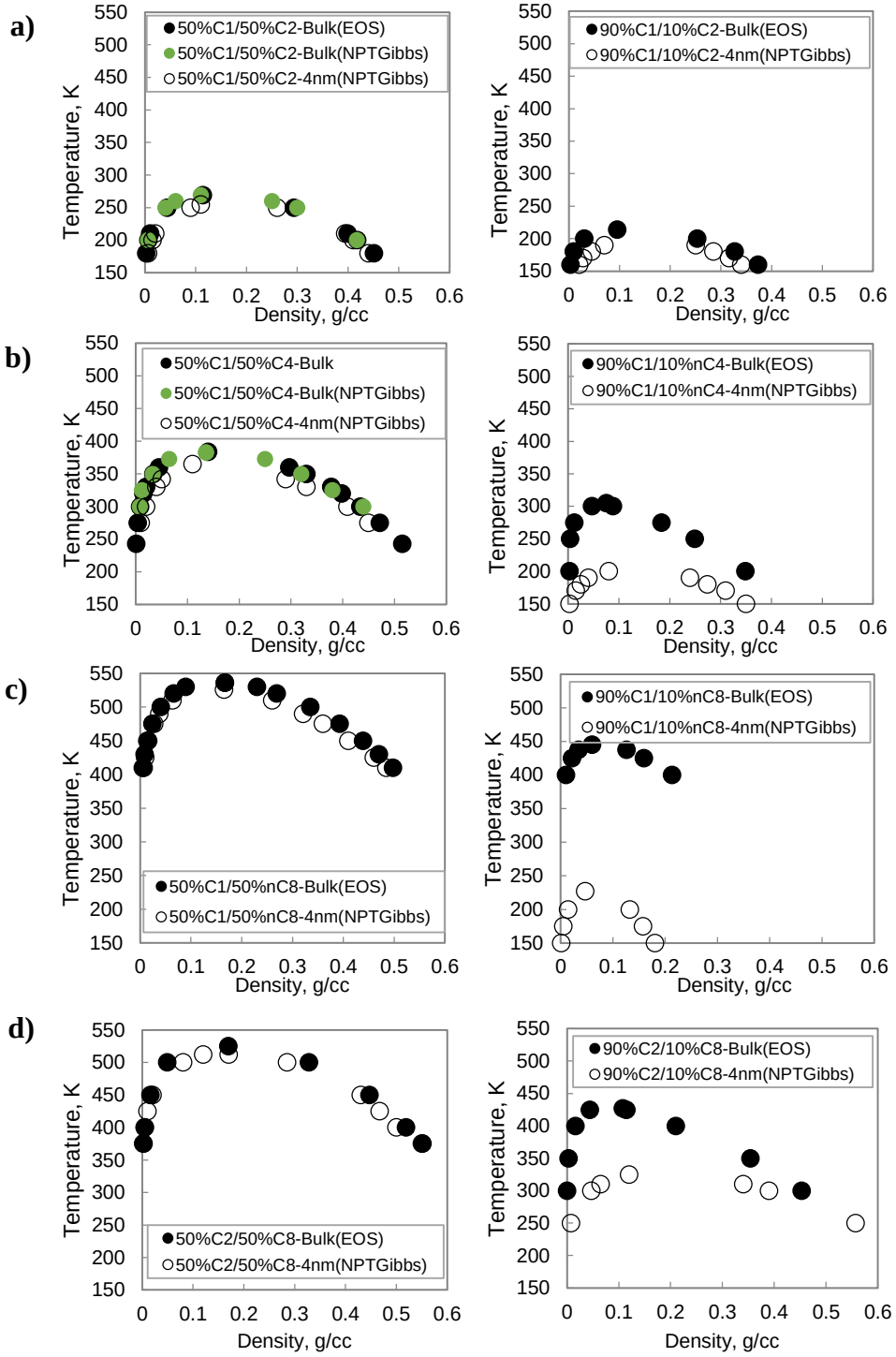

Figure 3.1: Phase diagrams of a) methane/ethane b) methane/n-butane c) methane/n-octane d) ethane/n-octane in bulk extracted from Peng-Robinson equation of state (filled circles) and in 4nm from NPT-Gibbs simulations (empty circles). Diagrams on left are for 50%/50% and on right are for 90%/10% molar compositions.

For the methane/n-butane mixture, the shift in the equimolar case, as in methane/ethane case, seems negligible; however in the 90%/10% case the shift is considerable. The diagrams of methane/n-octane follow the same trend and show no significant shift from bulk for 50%/50% but a great shift for 90%/10%. The shift in 90%/10% case of ethane/n-octane although remarkable, is not as striking as for its counterpart in methane/n-octane. In conclusion, the shifts seen for equimolar binary mixtures studied here are negligible; however, it appears that for binary mixtures with methane, the amount of shift becomes increasingly larger as the second component becomes heavier and longer-chained. Ethane is closer to n-octane in length of chain and number of carbons than methane is, and therefore its confined diagram shift is not as great as methane/n-octane.

To investigate whether this finding would hold for multi-component mixtures, simulations for ternary mixtures of methane, n-butane and n-octane are performed and studied. The molar percentage of n-butane is kept a constant 50% to see the effect of increasing the molar percentage of light component methane from 10% up to 40%. Results are shown in Figure 3.2. The least shift in the confined phase diagrams belongs to the 10% methane case; the mixture with the least percentage of methane. The greatest shift is seen for the least percentage of heavy component n-octane and therefore high percentage of methane. As such, the effect of methane in shifting the phase diagram in confinement is obvious, even in ternary mixtures. This means the addition of more components into the mixture does not seem to mask the effect of methane on the phase diagram.

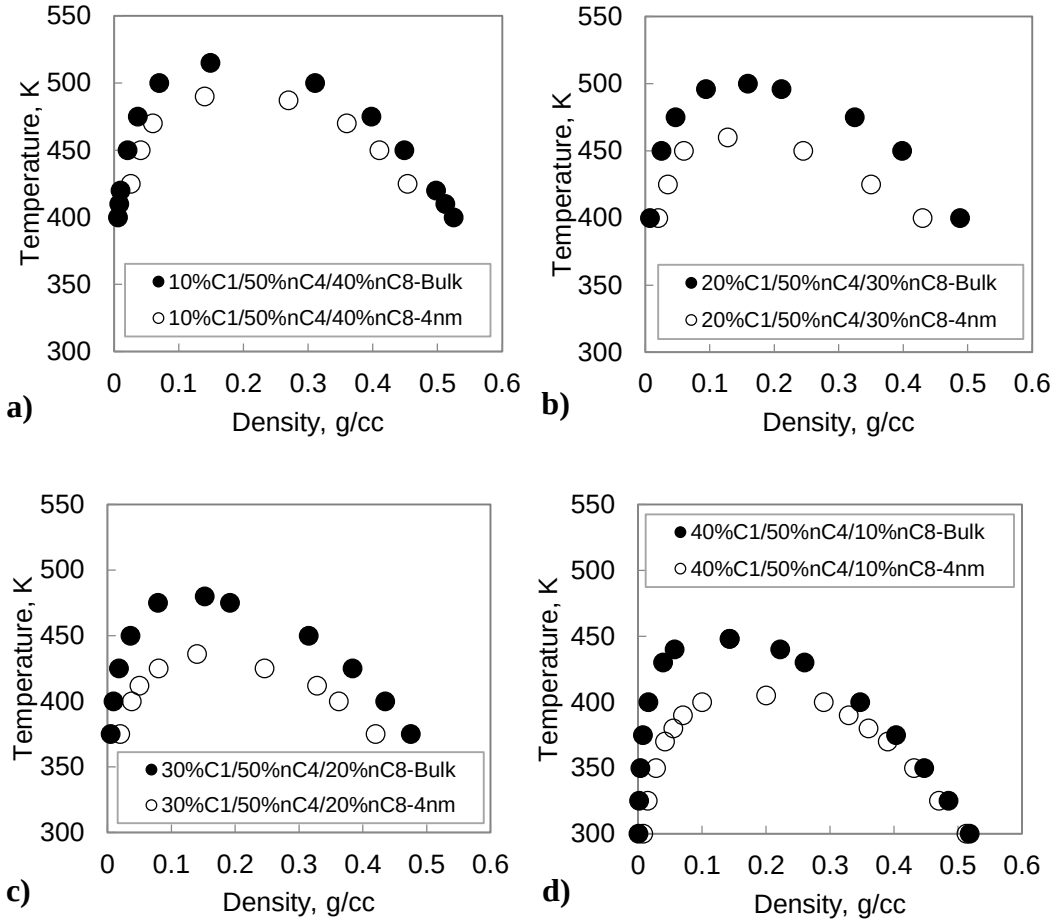

Figure 3.2: Phase diagrams of ternary methane/n-butane/n-octane mixtures of a) 10%/50%/40% b) 20%/50%/30% c) 30%/50%/20% d) 40%/50%/10% molar compositions in bulk state extracted from Peng-Robinson equation of state (filled circles) and NPT-Gibbs simulations (empty circles)

Figures 3.1 and 3.2 show the critical point temperature and saturation density shifts of mixtures in confinement. Tables 3.1 and 3.2 show the vapor and liquid saturation pressure shifts due to confinement. These tables show the saturation pressures at a few temperatures, however the trend is clear; unlike critical temperatures, saturation and therefore critical pressures increase in confinement. For the binary mixture (Table 3.1), the change in vapor saturation pressure due to confinement is significant for both cases but is more pronounced for the higher percentage of methane (90% C_1 – 10% n-C_4). The liquid saturation pressures in confinement for both cases are elevated at approximately the same extent. For the ternary mixture (Table 3.2), as also seen in the binary mixture, the increase in vapor saturation pressure due to confinement is also greater for the case with higher percentage of methane. Also, the liquid saturation pressures in confinement are slightly elevated.

Table 3.1: Vapor and liquid saturation pressures of two binary mixtures of methane and n-butane in bulk state (obtained from Peng-Robinson equation of state) and 4nm confinement (obtained from NPT-Gibbs ensemble molecular simulations).

	Bulk State		4nm Confinement	
Temperature, K	$P_v^{sat.}$,psi	$P_L^{sat.}$,psi	$P_v^{sat.}$,psi	$P_L^{sat.}$,psi
50% C_1 – 50% n-C_4				
275	33	1328	160	1650
300	79	1509	275	1820
330	192	1621	572	1970
342	267	1627	790	1900
90% C_1 – 10% n-C_4				
150	0.02	140	12	260
170	0.20	311	404	420
180	0.54	435	408	527
190	1.40	591	550	574

Table 3.2: Vapor and liquid saturation pressures of two ternary mixtures of methane, n-butane and n-octane in bulk state (obtained from Peng-Robinson equation of state) and 4nm confinement (obtained from NPT-Gibbs ensemble molecular simulations).

	Bulk State		4nm Confinement	
Temperature, K	$P_v^{sat.}$,psi	$P_L^{sat.}$,psi	$P_v^{sat.}$,psi	$P_L^{sat.}$,psi
10% C_1 – 50% n-C_4 – 40% n-C_8				
425	73	624	195	683
450	132	689	289	770
470	204	735	390	850
40% C_1 – 50% n-C_4 – 10% n-C_8				
300	4	1319	67	1370
325	11	1464	135	1510
350	29	1563	253	1620

3.4 REVISITING MIXING RULES

A key component to current reservoir simulators is the phase behavior and reservoir fluid properties package. Such a package is used to model and match reservoir fluids previously analyzed in the laboratory as accurately as possible to be used for fluid behavior predictions and improvement of our understanding of exploitation schemes. The equations of state most widely used in these packages are Soave-Redlich-Kwong (1972) and Peng-Robinson (1976) (Equation 3.1) which are in fact, modifications and improvements to the original van der Waals equation of state (1873). Soave (1972) also implemented the Pitzer acentric factor ω which is a measure of the non-sphericity of molecules, to be used in the Redlich-Kwong equation of state. These equations use critical parameters to describe and predict fluid properties such as pressure and density and vice versa. The Peng-Robinson equation of state is described as below:

$$P = \frac{RT}{V - b} - \frac{a\alpha}{V(V + b) + b(V - b)} \tag{3.1}$$

where

$$\alpha = \left(1 + k\left[1 - \left(\frac{T}{T_c}\right)^{0.5}\right]\right)^2 \tag{3.2a}$$

$$k = 0.37464 + 1.5422\omega - 0.26922\omega^2 \tag{3.2b}$$

$$a = 0.45724\frac{R^2T_c^2}{P_c} \quad , \quad b = 0.0778\frac{RT_c}{P_c} \tag{3.3c}$$

For fluids of two or more components, quadratic mixing rules are used to obtain critical parameters and construct phase diagrams. Mixing rules relate the properties of

single components to their mixtures. The simplest mixing rule is the linear average of the parameters a and b in the equation of state of the present components in the mixture:

$$a = \sum_{i=1} x_i a_i \quad , \quad b = \sum_{i=1} x_i b_i \tag{3.3}$$

Kay's rule is another mixing rule in which the critical parameters of a mixture are calculated as the molar averages of the critical parameters of the mixture's components:

$$T_c = \sum_{i=1} x_i T_{c_i} \quad , \quad P_c = \sum_{i=1} x_i P_{c_i} \tag{3.4}$$

Both linear averaging method and Kay's rule do not account for interactions between unlike components in a mixture and therefore are oversimplified.

Piper et al. (1993) developed a new correlation from 1482 data points of various lean sweet to rich acidic reservoir fluids. This correlation provides accurate estimates of the gas compressibility factor and critical parameters for a mixture. In this correlation, the pseudo-critical parameters are described as below.

$$T_{pc} = \frac{K^2}{J} \quad , \quad P_{pc} = \frac{T_{pc}}{J} \tag{3.5}$$

where

$$K = -0.39741 + 0.98211 \left[\sum_{i=1} x_i \left(\frac{1.8 T_{c_i}}{\sqrt{P_{c_i}}} \right) \right] \tag{3.6a}$$

$$J = 0.052073 + 0.85101 \left[\sum_{i=1} x_i \left(\frac{1.8 T_{c_i}}{P_{c_i}} \right) \right] \tag{3.6b}$$

Since the phase diagrams and therefore critical parameters of pure methane, n-butane and n-octane in 4nm pore width were obtained in chapter 2, the described mixing rules can be used to obtain estimates of the critical parameters of a binary mixture of, for instance, equimolar methane and n-butane in 4nm wide confinement. Table 3.3 shows the critical parameters of equimolar binary mixture of methane and n-butane in 4nm confinement, obtained from the linear average method, Kay's rule, and Piper et al. correlation. Also shown in the table are the critical parameters of the mixture itself in a 4nm wide pore obtained from this chapter's described method of NPT-Gibbs ensemble in Monte Carlo.

3.5 DISCUSSION

The four components chosen were aimed to represent lightest, light, intermediate and heavy *n*-alkanes. In multi-component systems, unlike single components, composition plays a central role in the phase diagram of bulk systems. In the confinement of such systems, due to selectivity of the wall, the role of composition becomes more highlighted. The aim of this chapter was to study this area as well as the extent of the phase diagram shift and also to identify the most influential component. This study would ultimately help in the prediction of phase diagram shape and approximation of critical point location of oil and natural gas existing in the nanopores of shale.

For equimolar *n*-alkane binary systems, the shift in phase diagram, perhaps for all intents and purposes, is negligible. For binary systems rich in the lighter component, as the difference between numbers of carbons in the alkane chain of the two components becomes greater, so does the phase diagram shift. Perhaps one reason for this finding is

Table 3.3: Comparison of critical parameter of a binary mixture obtained from four different methods. Single component critical parameters are obtained from Peng-Robinson equation of state (for bulk state) and GCMC simulations (for 4nm confinement, [chapter 2]). Mixture critical parameters are obtained from linear average, Kay's rule and Piper et al. method for 4nm confinement parameters and also the mixture itself in a 4nm confinement from NPT-Gibbs ensemble Monte Carlo.

	Single Components				50%C_1-50%n-C_4 Mixture			
	Bulk State		4nm Confinement		4nm Confinement			
	C_1	n-C_4	C_1	n-C_4	Linear Average	Kay's Rule	Piper et al.	Mixture in MC
T_c, K	191	425	172	360	307.5	266	364.5	365
P_c, psia	667.2	549.3	3217	2612	3214.5	2914.5	1836	1306

that, the pore wall attracts heavier components, leaving the interior for the lighter component. Since the number of molecules in the system is constant, this would also leave the bulk fluid box with more of the lighter component and less of the heavier component. Then, this would cause the phase diagram obtained from bulk fluid box to appear lower, and more similar to the lighter component. Phase diagram of a light component lies well below that of a heavy component. Unlike critical temperature, vapor saturation pressures are elevated in confinement. This elevation is greater for the mixture rich in lighter component. Results show that the liquid saturation pressure also increases due to confinement, although to a much less extent than vapor saturation pressure. The increases in saturation pressures may also be due to molecule packing effects.

For ternary *n*-alkane systems, the effect of increasing the molar percentage of light component was studied. It is found that the decisive role of the light component on the phase diagram is not masked by other components in the mixture. However, its role seems to be diminishing with the addition of those components. Vapor saturation pressures also increase due to confinement, especially for the mixture rich in lighter component. The liquid saturation pressures are only slightly affected by confinement. The trend seen in ternary mixture saturation pressures are consistent with those of binary mixtures.

Table 3.3 shows that for the equimolar binary mixture studied in confinement, different mixing rules yield fairly different sets of critical parameters, which are also quite different than those obtained from the NPT-Gibbs ensemble method. The linear averaging method and Kay's rule seem to be underestimating critical parameters in respect to the other methods. The NPT-Gibbs ensemble Monte Carlo yields a unique set of critical

parameters and takes into account the interaction of unlike molecules in a mixture, as well as the interactions between the mixture molecules and the wall.

CHAPTER IV

PORE GEOMETRY EFFECT ON ADSORPTION

In chapter 1, single component n-alkanes were studied in confinement of homogeneous slit geometry pores. In this chapter, adsorption traits of methane in cylindrical pore with graphite wall (carbon nanotube) will be studied in several conditions and compared to its equivalent slit-shaped results. The observed differences are discussed and conclusions are made. These carbon nanotubes can be analogous to pore throats in the shale microstructure.

4.1 INTRODUCTION

In the vast area of fluid confinement, it is inevitable to encounter the aspect of confinement geometry. Pores of shale are found in various sizes as well as shapes (e.g. spheres, nanohorns). In particular, one geometry is of utmost importance; the cylindrical shape. This pore structure, evident from SEM images, can be found independently or connecting two separate pores to each other, also known as pore throats. As with any confinement, cylindrical pores force their confined fluid to deviate in behavior with respect to bulk.

In cylindrical pores, characteristic phase transitions and capillary condensation have been investigated by Peterson et al. (1990), Peterson and Gubbins (1987), Heffelfinger et al. (1987), Panagiotopoulos (1987b) and Evans and Tarazona (1984) as well as more recently by Long et al. (2013), Huang et al. (2012 and 2009), Gordillo et al. (2006), Striolo et al. (2004). Capillary condensation is described as a state in which a fluid

that is normally in gas phase in bulk state condenses to form a liquid phase inside a narrow capillary. Evans and Tarazona (1984) studied this phenomenon in slit-shaped pores with the help of density functional theory. The three other mentioned groups, studied capillary condensation in cylindrical pores with GCMC, molecular dynamics (MD) and Gibbs MC and, found concurring results. In the MD path, a long cylindrical pore containing a fixed number of molecules at a high temperature (supercritical) is slowly temperature-quenched, during which the fluid is phase separated into two liquid-like and gas-like regions. At this point, both regions will have an adsorbed layer closest to the wall, although the liquid-like phase (condensation) may have several such layers depending on the pore diameter. In another interesting procedure, Peterson and Gubbins (1987) investigate phase transitions and locate capillary critical points with the help of adsorption isotherms. These isotherms, were obtained separately by Mean Field Theory (MFT) and GCMC simulations. Points on the isotherms were found by increasing (for adsorption) and decreasing (for desorption) the chemical potential. When the temperature is well below capillary critical point, the two branches of gas and liquid phases are separated. At temperatures closer to the critical point, the branches approach one another. At higher temperatures, only a single continuous branch exists, showing no hysteresis.

In all studies, condensation of the fluid inside the capillary is reported to be taking place at lower temperatures than in bulk. Apart from pure science, the practical impact of capillary condensation in coal was studied by Astakhov and Shirochin (1990).
In that experimental study, they found that “capillary-like” condensation happens in coal pores and lowers the strength of those pores.

One of the first steps to understanding phase behavior in confinement of a given geometry is to study the fluid's layering and density profile inside the pore. In this chapter, density profiles of methane in single-wall carbon nanotubes (SWCNT) of various pore diameters are obtained from GCMC simulations. Results are compared to their corresponding slit-shaped pores.

4.2 SIMULATION SETUP

Grand canonical Monte Carlo simulations are used to simulate methane in SWCNT at a temperature of 353K. Simulations are conducted in one box, containing the nanotube, at fixed temperature, volume and chemical potential. Two values of chemical potential corresponding to two values of pressure are chosen for this study. Each simulation is allowed to evolve with 4×10^6 moves of insertion/deletion and translation.

The fluid parameters can be found in Table 2.1. A single-wall carbon nanotube is built by rolling up a sheet of graphene such that the edge atoms bind to one another seamlessly (Kolasinski, 2012). A CNT is characterized by its chiral vector C:

$$\mathrm{C} = \mathrm{n}a_1 + \mathrm{m}a_2 \tag{4.1}$$

where n and m are integers and a_1 and a_2 are the unit vectors of graphene. When $\mathrm{n} = \mathrm{m}$, armchair nanotube is formed and when $\mathrm{m} = 0$, the zigzag structure is formed. Chiral nanotubes can be formed anywhere in between these two cases. In addition to the arrangement, values of n and m also determine the electronic structure of the nanotube and diameter. In this chapter, the armchair structure is used for the SWCNT.

The diameter of a CNT in nanometers is calculated by:

$$d = 0.0783\sqrt{n^2 + nm + m^2} \quad (4.2)$$

The force field used for the nanotube is Walther et al. 2001 (Walt2001) which assumes Lennard-Jones interactions and values of σ=3.85 and ε=52.87 as its parameters. The densities of methane are obtained with the help of a molecular visualization program.

First, the effect of pressure on adsorption in a 3nm diameter CNT is studied. Then, the result of simulations in 3nm CNT is compared to that in a 3nm wide slit-pore. Lastly, the effect of CNT pore size on adsorption is studied with pores of 1, 3 and 5nm diameter.

4.3 RESULTS

Figure 4.1 is a snapshot of the simulation of methane in a 3nm diameter CNT at 353K. Figure 4.2 shows the density profiles of methane in a CNT with a diameter of 3nm, at two chemical potentials corresponding to pressures of 3200psia (high) and 30000psi (very high) at bulk. Both profiles indicate the existence of four dense concentric rings of methane molecules in the 3nm CNT.

Figure 4.3 demonstrates the density profile of methane in a CNT and graphite slit-pore. For the purpose of comparison, temperature, bulk pressure and pore size are equal for both cases.

Figure 4.4 shows methane density profile in 1, 3 and 5nm diameter CNT at 353K temperature and 3200psi bulk pressure.

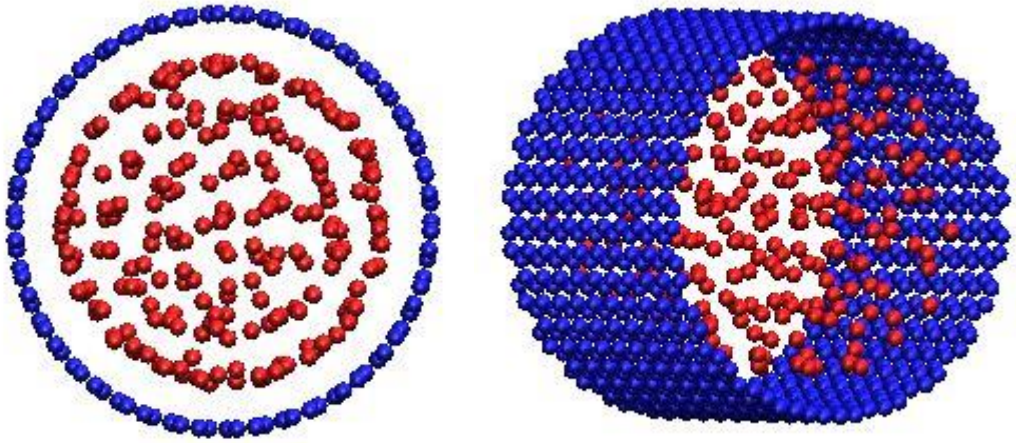

Figure 4.1: Snapshot of methane (red spheres) in 3nm diameter CNT (blue structure) at 353K temperature and 32000psi pressure.

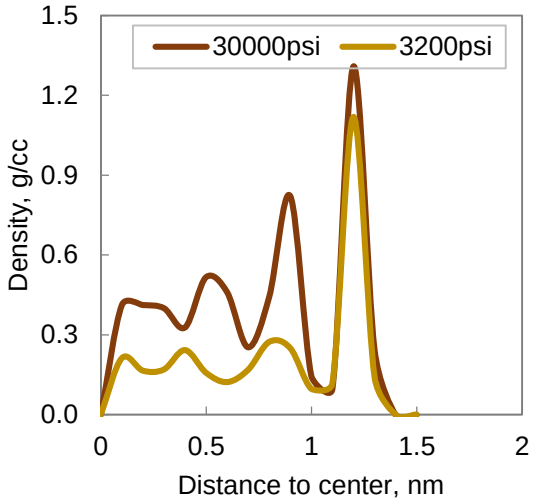

Figure 4.2: Density profiles of methane in 3nm diameter CNT at two different bulk pressures of 3200 and 30000psi and 353K temperature. Four distinct rings of dense molecules are observable.

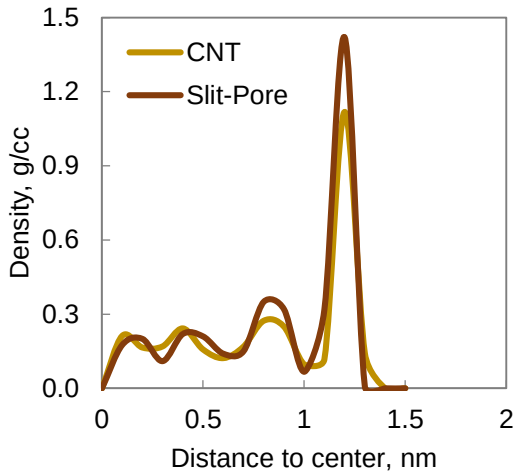

Figure 4.3: Density profiles of methane in 3nm diameter CNT and b) 3nm width graphite slit-pore, both at 3200psi bulk pressure and 353K temperature. In the slit-pore, amount of methane gradually decreases starting from the wall to the center.

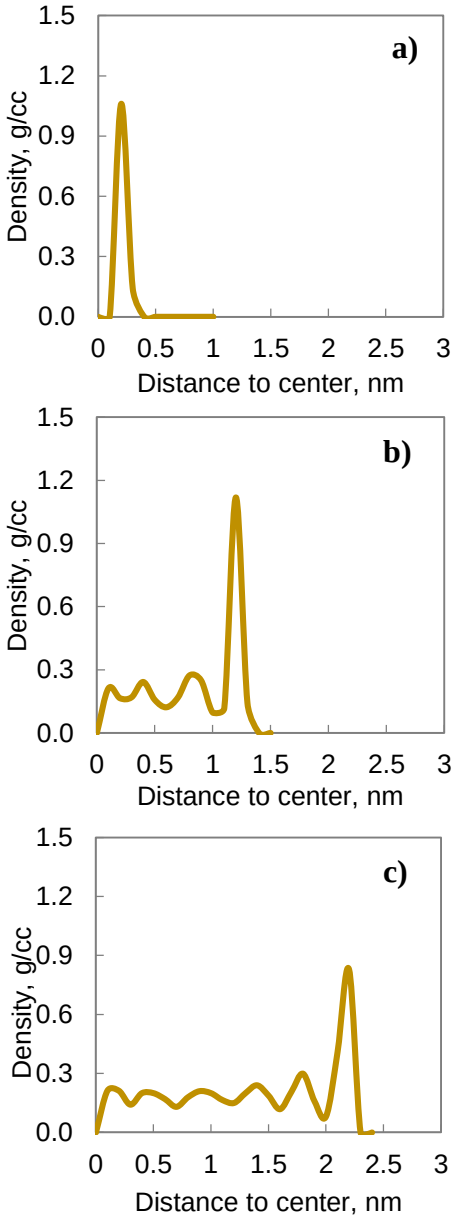

Figure 4.4: Density profiles of methane in a) 1nm b) 3nm and c) 5nm diameter CNT all at 3200psi bulk pressure and 353K temperature.

4.4 DISCUSSION

The effect of pressure on methane adsorption in CNT is shown in Figure 4.2. Note that in this figure, only half the pore is demonstrated. At both pressures, four distinct peaks can be observed. The highest peak corresponds to the layer closest to the CNT wall (outermost layer) indicating a dense adsorbed phase. In addition, the densities between the concentric rings are nonzero, because molecules are constantly moving between the rings. At the very high pressure, the densities have all increased, especially the second layer closest to the wall. We can conclude that as the pressure is increased, the outermost layer becomes saturated. Then, the saturation follows for the next layers. This can be an indication of capillary condensation.

In Figure 4.3 the effect of pore geometry on adsorption is shown. The density profiles are very similar and in both the CNT and slit-pore, four distinct molecule layers are apparent. The density profile inside the slit-pore is gradually dampening from the outermost to the innermost layers. This is not entirely the case for the CNT, since there appears to peaks with nearly equal heights in inner layers. The outermost layer in the slit-pore is denser than that of the CNT.

Figure 4.4 shows how the density profile changes from a 1nm in diameter CNT to a 5nm in diameter. In a 1nm in diameter CNT, methane molecules can only form a single ring. In a 3nm and 5nm in diameter CNT, molecules form 4 and 6 concentric rings, respectively. Apart from the outermost ring, all other rings seem to have approximately equal densities. Also, as the CNT becomes wider, the outermost layer (adsorbed layer), becomes less dense.

CHAPTER V

CONCLUSIONS AND FUTURE WORK

In this thesis, the study of the effect of confinement on fluids was conducted by the use of molecular simulations. Throughout the thesis, confinement is assumed to be of slit-pore geometry, unless stated otherwise. This study began with single component fluids and their density profiles. Density profiles have proved to be very useful in forming our understanding of the fluid behavior in confinement. For the single component fluids studied here, the grand canonical ensemble in the Monte Carlo simulations followed by histogram reweighting was used. Phase diagrams of the three fluids (methane, n-butane and n-octane) obtained in various pore sizes from this method showed that at approximately 12nm pore thickness, the fluid approaches bulk state behavior and the effect of confinement becomes virtually negligible. In pores narrower than this threshold, the confinement effect cannot be neglected. In fact, the effect of confinement is much more intense on the vapor branch than on the liquid branch. In addition, critical parameters of the fluids studied are extracted from the obtained phase diagrams to be used in mixing rules.

Obviously, single component fluids virtually never exist in oil and gas reservoirs and shale resources. Therefore, in the second chapter, the study was expanded to binary and ternary mixtures. For this section, the Gibbs ensemble was utilized within the Monte Carlo realm. As in single components, phase diagrams of confined binary and ternary mixtures also showed suppression compared to their bulk state, although in a more

uniform fashion than those of single components in terms of vapor and liquid branches. Composition becomes a key issue in phase diagrams of mixtures. Eight binary and four ternary mixtures consisting of components methane (as light component), ethane, n-butane and n-octane (as heavy component) were studied. It was found that with the increase of the light component in the mixture, the phase diagram becomes suppressed greater. This can be explained due to the higher selectivity of the wall towards larger and heavier molecules. Such molecules occupy the layer closest to the wall, allowing lighter components to occupy more inner spaces of the pore. Phase transitions begin from these inner spaces and therefore the light component will play a decisive role in phase transitions. Since phase diagram curves of light molecules themselves are located at lower temperatures and densities than in heavy components, a greater percentage of light components in the mixture will suppress the mixture phase diagram curve to lower temperatures and densities.

Three mixing rules were studied to obtain critical parameters of mixtures in confinement. These mixing rules proved to yield different results than those obtained from applying the NPT-Gibbs ensemble Monte Carlo to the mixture. Seemingly, current mixing rules are not able to describe fluid behavior in confinement.

In conclusion, the deviated phase diagrams obtained for single and multi-component fluids do not obey well-known equations of state and therefore urge for the development of new models and correlations that would reliably describe fluid behavior in confinement. These correlations must take into account factors such as pore size and molecule-wall interactions. The incorporation of such correlations into reservoir fluid

simulator packages, would yield more accurate descriptions of fluid behavior and improve our understanding of extraction scenarios and outcomes.

Although the majority of this thesis assumed slit-pore geometry to confinement, in the last chapter the results obtained from fluid adsorption in SWCNT showed qualitative similarity to those obtained from slit-pore geometry. Therefore, in future work, it is expected that, for example, phase diagrams of fluid in nanotube geometry would yield similar results in terms of phase diagram suppression to those in slit-pore geometry. The CNT studied here seemed to hold fluid in a high adsorbed layer closest to the tube wall followed by inner concentric rings with nearly identical densities. This is opposed to the slit-pore forming a dampening density profile across the pore width. It can be concluded that condensation happens earlier in a CNT than in a slit-pore. Perhaps this would cause the phase diagrams of fluid to be suppressed greater (phase transitions happening in lower temperatures) than in the slit-pore, under similar conditions.

REFERENCES

Adesida, A. G., Akkutlu, I. Y., Resasco, D. E., Rai, C. S.2011. Characterization of Barnett Shale Kerogen Pore Size Distribution using DFT Analysis and Grand Canonical Ensemble Monte Carlo. Paper SPE 147397 presented at the SPE Annual Technical Conference and Exhibition, Denver, Colorado, USA, 30 October – 2 November

Ambrose, R. J., Hartman, R. C., Diaz-Campos, M., Akkutlu, I. Y., Sondergeld, C. H. 2010. New Pore-Scale Considerations for Shale Gas in Place Calculations. Paper SPE 131772 presented at the SPE Unconventional Gas Conference, Pittsburgh, Pennsylvania, USA, 23-25 February.

Anderson, H. 1986. Metropolis, Monte Carlo, and the MANIAC. *Los Alamos Science*.

Astakhov, A. V., Shirochin, D. L. 1990. Capillary-Like Condensation of Sorbed Gases in Coals. *Fuel* **70**: 51-56.

Bustin, R. M., Bustin, A. M. M., Cui, X., Ross, D. J. K., Murthy Pathi, V. S. 2008. Impact of Shale Properties on Pore Structure and Storage Characteristics. Paper SPE 119892 presented at the SPE Shale Gas Production Conference, Fort Worth, Texas, USA, 16-18 November

Clarkson, C. R., Solano, N., Bustin, R. M., Bustin, A. M. M., Chalmers, G. R. L., He, L., Melnichenko, Y. B., Radlinski, A. P., Blach, T. P. 2013. Pore Structure Characterization of North American Shale Gas Reservoirs using USANS/SANS, Gas Adsorption and Mercury Intrusion. *Fuel* **103**: 606-616

Cracknell, R. F., Nicholson, D., Quirke, N. 1994. A Grand Canonical Monte-Carlo Study of Lennard-Jones Mixtures in Slit Pores; 2: Mixtures of Two Centre Ethane with Methane. *Molecular Simulations* **13**: 161-175.

Cracknell, R. F., Nicholson, D., Tennison, S. R., Bromhead, J. 1995. Adsorption and Selectivity of Carbon Dioxide with Methane and Nitrogen in Slit-Shaped Carbonaceous Micropores: Simulation and Experiment. *Adsorption* **2**: 193-203.

Curtis, M. E., Ambrose, R. J., Sondergeld, C. H., Rai, C. S. 2011a. Transmission and Scanning Electron Microscopy Investigation of Pore Connectivity of Gas Shales on the Nanoscale. Paper SPE 144391 presented at the SPE North American Unconventional Gas Conference and Exhibition, The Woodlands, Texas, USA, 14-16 June.

Curtis, M. E., Ambrose, R. J., Sondergeld, C. H., Rai, C. S. 2011b. Investigation of the Relationship between Organic Porosity and Thermal Maturity in the Marcellus

Shale. Paper SPE 144370 presented at the SPE North American Unconventional Gas Conference and Exhibition, The Woodlands, Texas, USA, 14-16 June.

Diaz-Campos, M., Akkutlu, I. Y., Sigal, R. F. 2009. A Molecular Dynamics Study on Natural Gas Solubility Enhancement in Water Confined to Small Pores. Paper SPE 124491 presented at the SPE Annual Technical Conference and Exhibition, New Orleans, Louisiana, USA, 4-7 October.

Evans, R., Tarazona, P. 1984. Theory of Condensation in Narrow Capillaries. *Physical Review Letters* **52** (7): 557-560.

Firouzi, M., Wilcox, J. 2012. Molecular Modeling of Carbon Dioxide Transport and Storage in Porous Carbon-Based Materials. *Microporous and Mesoporous Materials* **158**: 195-203

Ferrenberg, A. M., Swendsen, R. H. 1989. Optimized Monte Carlo Data Analysis. *Physical Review Letters* **63** (12): 1195-1198.

Frenkel, D. 2004. Introduction to Monte Carlo Methods. *NIC Series* **23**: 29-60.

Gelb, L.D., Gubbins, K.E., Radhakrishnan, R., Sliwinska-Bartkowiak, M. 1999. Phase Separation in Confined Systems. *Rep. Prog. Phys*. **62**: 1573-1659

Gordillo, M. C., Martinez-Haya, B., Romero-Enrique, J. M. 2006. Freezing of Hard Spheres Confined in Narrow Cylindrical Pores. *J. Chem. Phys.* **125**: 144702(1)-144702(4).

Heffelfinger, G. S., van Swon, F., Gubbins, K. E. 1987. Liquid-Vapor Coexistence in a Cylindrical Pore. *Molecular Physics* **61** (6):1381-1390.

Henderson, J. R. 1983. Potential-Distribution Theorem-Mechanical Stability and Kirkwood's Integral Equation. *Molecular Physics* **48** (4): 715-717.

Hoch, M. J. R. 2011. *Statistical and Thermal Physics: An Introduction*. Boca Raton, FL: Taylor and Francis Group.

Huang, H., Kwak, S., Singh, J. K. 2009. Characterization of Fluid-Solid Phase Transition of Hard-Sphere Fluids in Cylindrical Pore via Molecular Dynamics Simulation. *J. Chem. Phys.* **130**: 164511(1)-164511(6).

Huang, H., Singh, J. K., Lee, J., Kwak, S. 2012. Confining Effect of Carbon-Nanotube Configuration on Phase Behavior of Hard-Sphere Fluid. *Fluid Phase Equilibria* **318**: 19-24.

Jiang, J., Sandler, S.I., Schenk, M., Smit, B. 2005. Adsorption and Separation of Linear and Branched Alkanes on Carbon Nanotube Bundles from Configurational-Bias Monte Carlo Simulation. *Physical Review B* **72**(4): 045447

Kaneko, K., Cracknell, R. F., Nicholson, D. 1994. Nitrogen Adsorption in Slit Pores at Ambient Temperatures: Comparison of Simulation and Experiment. *Langmuir* **10** (12): 4606-4609.

Kang, S. M., Fathi, E., Ambrose, R. J., Akkutlu, I. Y., Sigal, R. F. 2011. Carbon Dioxide Storage Capacity of Organic-Rich Shales. *134583 SPE Journal* **16** (4).

Kierlik, E., Rosinberg, M., Finn, J. E., Monson, P. A. 1992. Binary Vapour Mixtures Adsorbed on a Graphite Surface: A Comparison of Mean Field Density Functional Theory with Results from Monte Carlo Simulations. *Molecular Physics* **75** (6): 1435-1454.

Kolasinski, K. W. 2012. *Surface Science: Foundations of Catalysis and Nanoscience, 3rd Edition*. John Wiley & Sons.

Liu, Y., Wilcox, J. 2012. Effects of Surface Heterogeneity on the Adsorption of CO_2 in Microporous Carbons with Surface Heterogeneity. *Environmental Science and Technology* **46** (3): 1940-1947.

Long, Y., Sliwinska-Bartkowiak, M., Drozdowski, H., Kempinski, M., Phillips, K. A., Palmer, J. C., Gubbins, K. E. 2013. High Pressure Effect in Nanoporous Carbon Materials: Effects of Pore Geometry. *Colloids and Surfaces A* **437**: 33-41.

Loucks, R. G., Reed, R. M., Ruppel, S. C., Jarvie, D. M. 2009. Morphology, Genesis and Distribution of Nanometer-Scale Pores in Siliceous Mudstones of the Mississippian Barnett Shale. *Journal of Sedimentary Research* **79**: 848-861.

Martin, M. G., Siepmann, J. I. 1998. Transferable Potentials for Phase Equilibria. 1. United-Atom Description of N-Alkanes. *J. Phys. Chem. B* **102**(14): 2569-2577.

Metropolis, N., Rosenbluth, A. W., Rosenbluth, M. N., Teller, A. H., Teller, E. 1953. Equation of State Calculations by Fast Computing Machines. *J. Chem. Phys.* **2**1: 1087-1092.

Mi, J., Tang, Y., Zhong, C., Li, Y. 2006. Prediction of Phase Behavior of Nanoconfined Lennard-Jones Fluids with Density Functional Theory based on the First-Order Mean Spherical Approximation. *J. Chem. Phys.* **124**(16): 144709(1)-144709(7).

Montgomery, S. L., Jarvie, D. M., Bowker, K. A., Pollastro, R. M. 2005. Mississippian Barnett Shale, Fort Worth Basin, North-Central Texas: Gas-Shale Play with Multi-

Trillion Cubic Foot Potential. *The American Association of Petroleum Geologists Bulletin* **89** (2):155-175

Mosher, K., He, J., Liu, Y., Rupp, E., Wilcox, J. 2013. Molecular Simulation of Methane Adsorption in Micro- and Mesoporous Carbons with Applications to Coal and Gas Shale Systems. *International Journal of Coal Geology* **109**: 36-44.

Panagiotopoulos, A. Z. 1987a. Direct Determination of Phase Coexistence Properties of Fluids by Monte Carlo Simulation in a new Ensemble. *Molecular Physics* **100** (1): 237-246.

Panagiotopoulos, A. Z. 1987b. Adsorption and Capillary Condensation of Fluids in Cylindrical Pores by Monte Carlo Simulations in the Gibbs Ensemble. *Molecular Physics* **62** (3): 701-719.

Panagiotopoulos, A. Z. 2000. On the Equivalence of Continuum and Lattice Models for Fluids. *J. Chem. Phys.* **112**(16): 7132-7137.

Peng, D., Robinson, D. B. 1976. A New Two-Constant Equation of State. *Industrial and Engineering Chemistry Fundamentals* **15** (1): 59-64.

Peterson, B. K., Gubbins, K. E. 1987. Phase Transitions in a Cylindrical Pore: Grand Canonical Monte Carlo, Mean Field Theory and the Kelvin Equation. *Molecular Physics* **62** (1): 215-226.

Peterson, B. K., Heffelfinger, G. S., Gubbins, K. E. 1990. Layering Transitions in Cylindrical Pores. *J. Chem. Phys.* **93** (1): 679-685.

Piper, L. D., McCain, W. D., Corredor, J. H. 1993. Compressibility Factors for Naturally Occurring Petroleum Gases. Paper SPE 26668 presented at the SPE Annual Technical Conference and Exhibition, Houston, Texas, USA, 3-6 October.

Potoff, J. J., Panagiotopoulos, A. Z. 1998. Critical Point and Phase Behavior of the Pure Fluid and a Lennard-Jones Mixture. *J. Chem. Phys.* **109** (24): 10914-10920.

Potoff, J. J., Panagiotopoulos, A. Z. 2000. Surface Tension of the Three-Dimensional Lennard-Jones Fluid from Histogram-Reweighting Monte Carlo Simulations. *J. Chem. Phys.* **112**(14): 6411-6415.

Potoff, J. J., Siepmann, J. I. 2001. Vapor-Liquid Equilibria of Mixtures Containing Alkanes, Carbon Dioxide, and Nitrogen. *AICHE Journal* **47** (7): 1676-1682.

Prausnitz, J. M. 1999. *Molecular Thermodynamics of Fluid Phase Equilibria*. Upper Saddle River, N.J.: Prentice Hall PTR

Rahmani Didar, B. 2012. Multi-Component Shale Gas-in-Place Calculations. M.Sc. thesis, University of Oklahoma, Norman, Oklahoma, USA.

Rahmani Didar, B. and Akkutlu, I.Y. 2013. Pore-Size Dependence of Fluid Phase Behavior and Properties in Organic-Rich Shale Reservoirs. Paper SPE 164099 presented at the SPE International Symposium on Oilfield Chemistry, The Woodlands, Texas, USA, 8-10 April.

Razmus, D. M., Hall, C. K. 1991. Prediction of Gas Adsorption in 5A Zeolites using Monte Carlo Simulation. *AICHE Journal* **37** (5): 769-779.

Singh, J. K., Errington, J. R. 2006. Calculation of Phase Coexistence Properties and Surface Tensions of n-Alkanes with Grand-Canonical Transition-Matrix Monte Carlo Simulation and Finite-Size Scaling. *J. Phys. Chem. B* **110**: 1369-1376.

Singh, S. K., Sinha, A., Deo, G., Singh, J. K. 2009. Vapor-Liquid Phase Coexistence, Critical Properties, and Surface Tension of Confined Alkanes. *J. Phys. Chem. C* **113**: 7170-7180.

Singh, S. K., Saha, A. K., Singh, J. K. 2010. Molecular Simulation Study of Vapor-Liquid Critical Properties of a Simple Fluid in Attractive Slit Pores: Crossover from 3D to 2D. *J. Phys. Chem. B* **114**: 4283-4292

Soave, G. 1972. Equilibrium Constants from a Modified Redlich-Kwong Equation of State. *Chemical Engineering Science* **27**: 1197-1203.

Sokolowski, S., Fischer, J. 1990. Lennard-Jones Mixtures in Slit-Like Pores: A Comparison of Simulation and Density-Functional Theory. *Molecular Physics* **71** (2): 393-412.

Sondergeld, C. H., Ambrose, R. J., Rai, C. S., Moncrieff, J. 2010. Micro-Structural Studies of Gas Shales. Paper SPE 131771 presented at the SPE Unconventional Gas Conference, Pittsburgh, Pennsylvania, USA, 23-25 February.

Steele, W. A. 1973. The Physical Interaction of Gases with Crystalline Solids. *Surface Science* **36** (1): 317-352.

Suleimenova, A., Bake, K. D., Ozkan, A., Valenza, J. J., Kleinberg, R. L., Burnham, A. K., Ferralis, N., Pomerantz, A. E. 2014. Acid Demineralization with Critical Point Drying: A Method for Kerogen Isolation that Preserves Microstructure. *Fuel* **135**: 492-497.

Tan, Z., Gubbins, K. E. 1992. Selective Adsorption of Simple Mixtures in Slit Pores: A Model of Methane-Ethane Mixtures in Carbon. *J. Phys. Chem.* **96** (2): 845-854.

Van der Waals, J. 1873. Over De Continuiteit Van Den Gas- En Vloeistoftoestand (On the Continuity of the Gas and Liquid State). Ph.D. Dissertation, Lieden University, The Netherlands.

Van Tassel, P., Davis, H. T., McCormick, A. 1996. Adsorption of Binary Mixtures in a Zeolite Micropore. *Molecular Simulation* **17** (4-6): 239-254.

Walther, J. H., Jaffe, R., Halicioglu, T., Koumoutsakos, P. 2001. Carbon Nanotubes in Water: Structural Characteristics and Energetics. *J. Phys. Chem. B* **105**: 9980-9987.

Zarragoicoechea, G. J. and Kuz, V. A. 2002. van der Waals Equation of State for a Fluid in a Nanopore. *J. of Physical Review E* **65** (2): 021110/1-021110/4.

Zarragoicoechea, G. J. and Kuz, V. A. 2004. Critical Shift of a Confined fluid in a nanopore. *Fluid Phase Equilibria* **220**: 7-9.